

Wave Particle Interactions in the Earth's Radiation Belts



J.-F. Ripoll ^{1a,1b}

(jean-francois.ripoll@cea.fr)



Collaborators:

V. Loridan^{1a}, T. Farges^{1a}, G. Cunningham², M. Denton^{3,4}, O. Santolík^{5,6}, D. Malaspina⁷, S. Thaller¹⁰, G. Reeves^{2,3}, D. Hartley⁸, W. S. Kurth⁸, C. A. Kletzing⁸, D. L. Turner¹⁰, J. F. Fennell⁹, M. G. Henderson², A. Y. Ukhorskiy¹⁰, A. Y. Drozdov¹¹, Y. Y. Shprits^{12,13}, J.S Cervantes Villa¹³, E. Botek¹⁴, V. Pierrard^{14,15}

DE LA RECHERCHE À L'INDUSTRIE

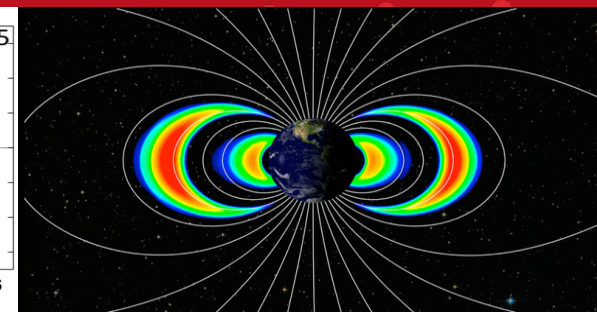
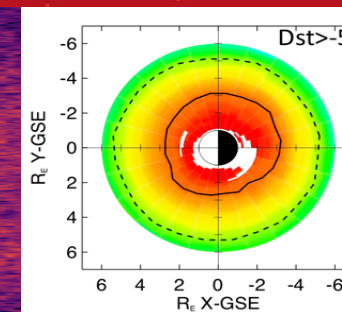
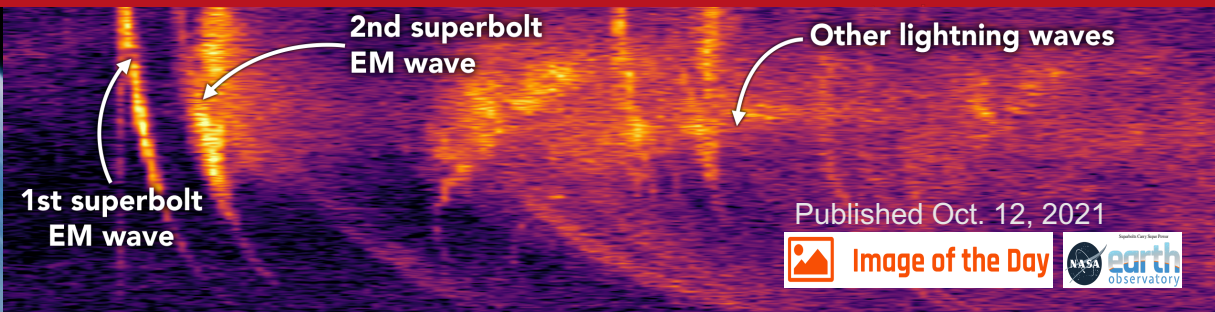
1a CEA, DAM, DIF, Arpajon, France
1b UPS, CEA, LMCE, France
2 Los Alamos National Laboratory
3 New Mexico Consortium
4 Space Science Institute, Boulder
5 Academic Science Czech Republic

6 Charles University, Prague
7 LASP
8 University of Iowa
9 Aerospace Corporation
10 Applied Physics Laboratory

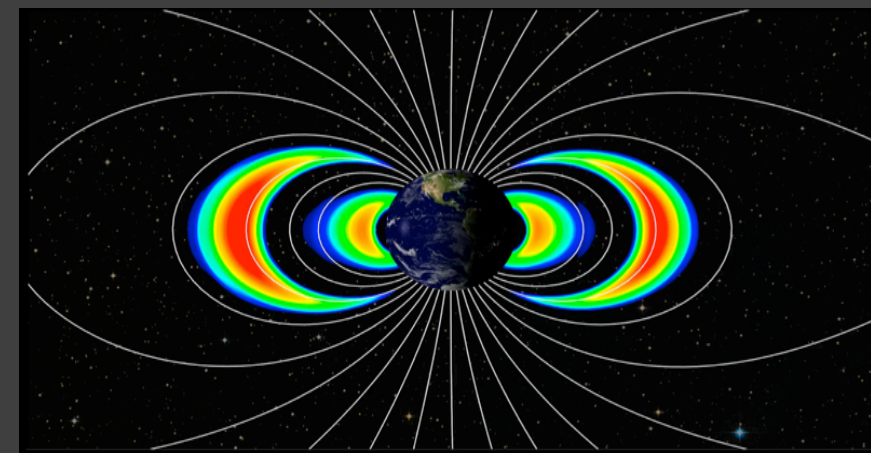
11 University of Minnesota
12 UCLA
13 Helmholtz Centre Potsdam, GFZ
14 BIRA, Belgium,
15 UC Louvain, Belgium



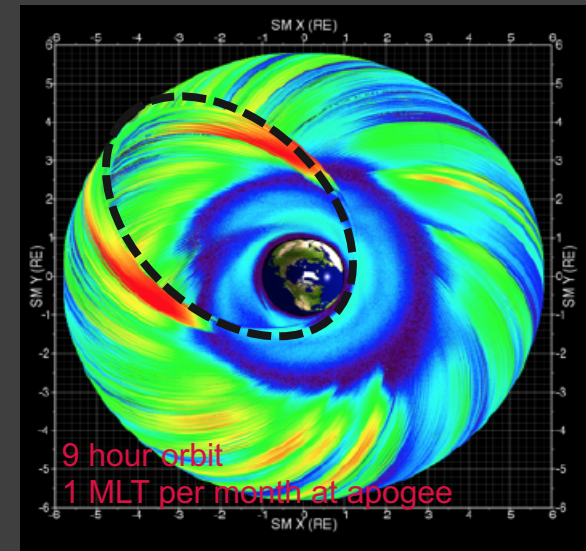
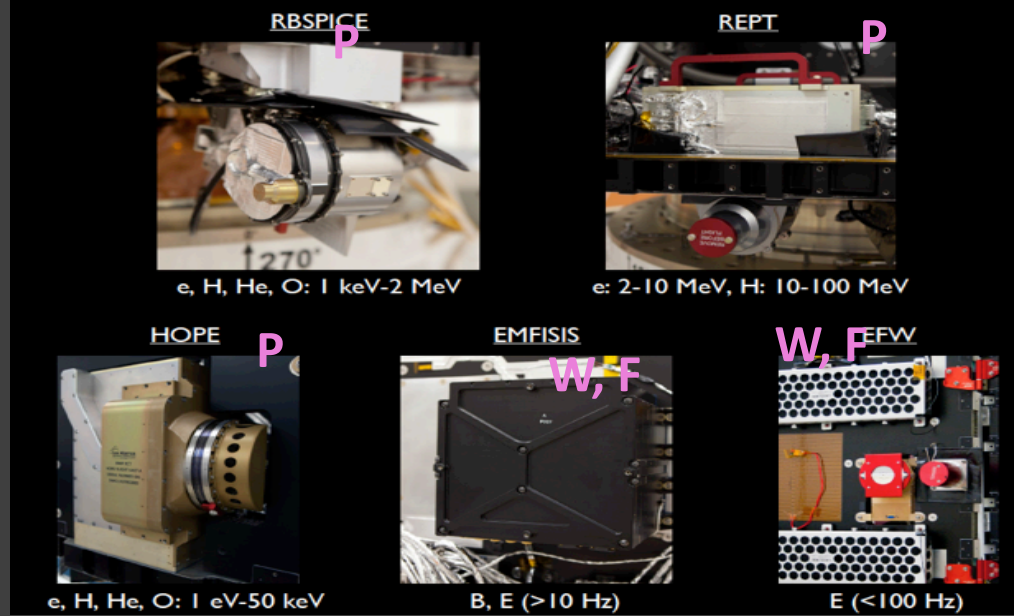
Credit: NASA



The radiation belts and the NASA Van ALLEN Probes (RBSP) mission (2012-2019)



Instrument suits for plasma (P), waves (W), and fields (F) on board the NASA Van Allen Probes



7 years of data (2012-2019)
from 2 s/c

Among the main NASA RBSP mission objectives:

- Better understand radiation belt physics
- Validate various models and explain x10 difference between simulations & observations

How to

- Using 2 s/c measuring **simultaneously** the ambient **wave** environment and the **radiation belts fluxes**
- Solve for wave-particle interactions using in-situ measurements

Motivation

Dynamics in the radiation belts is driven by wave particle interactions

Understand and compute the dynamics of the radiation belts

Objectives of the talk:

Show some recent examples of important WPI in the radiation belts from observations and simulations

Observations of WPI in the radiation belts

Cold electron plasma and whistler-mode waves

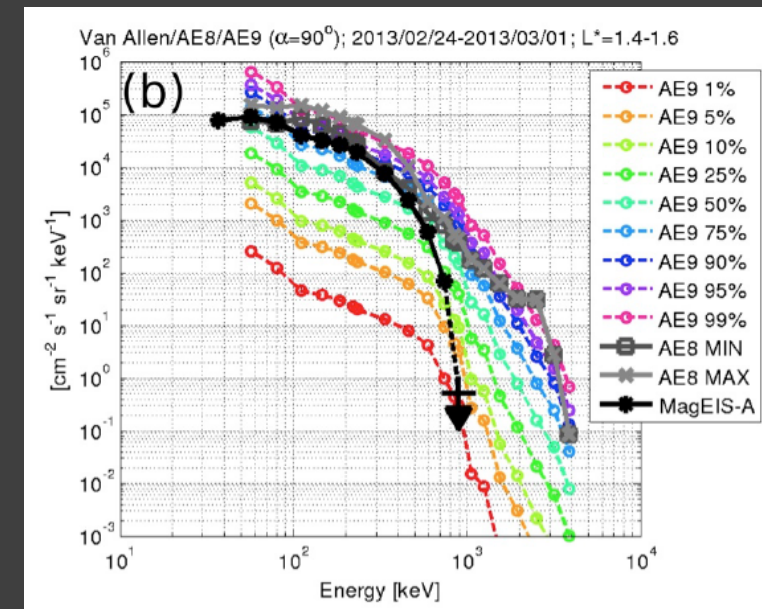
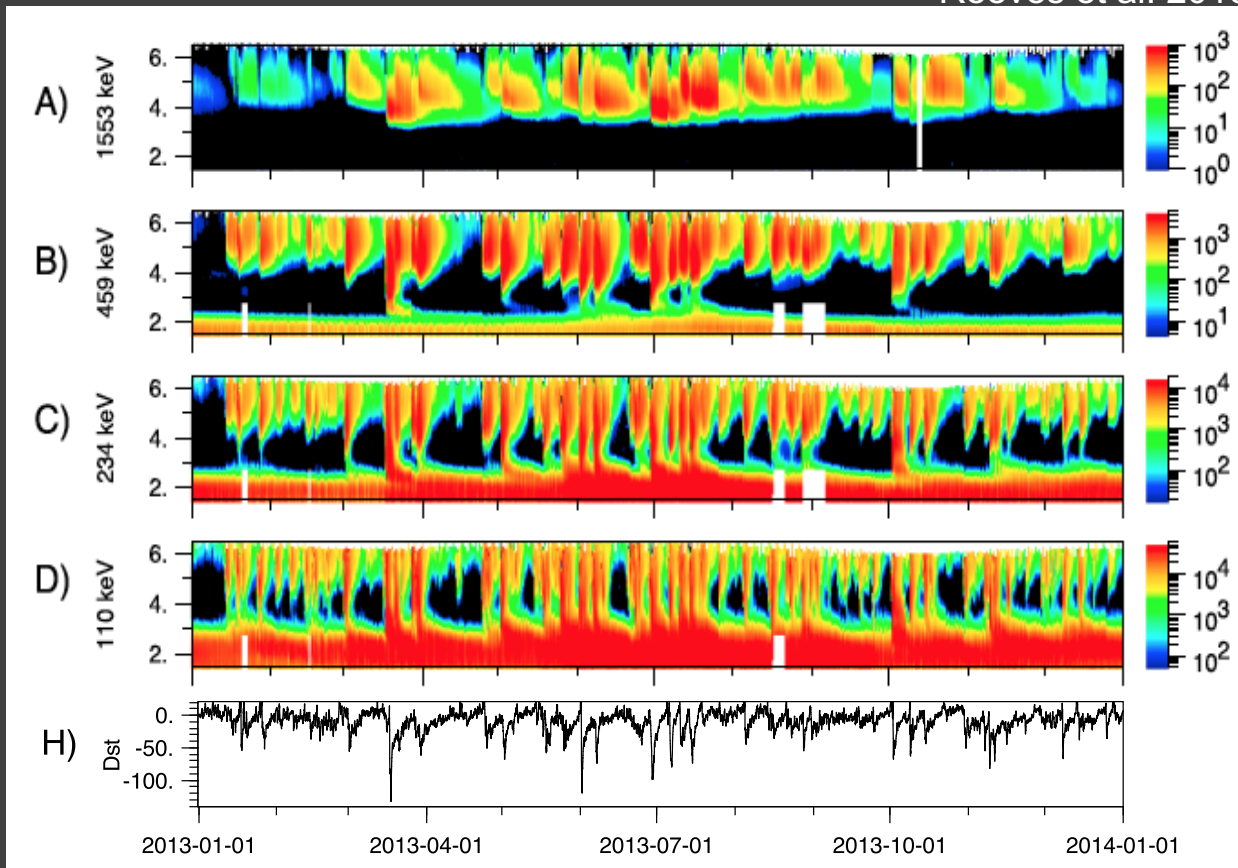
Event-driven WPI simulations of radiation belt dynamics

Conclusions and Perspectives



Observations of the radiation belts

Reeves et al. 2016

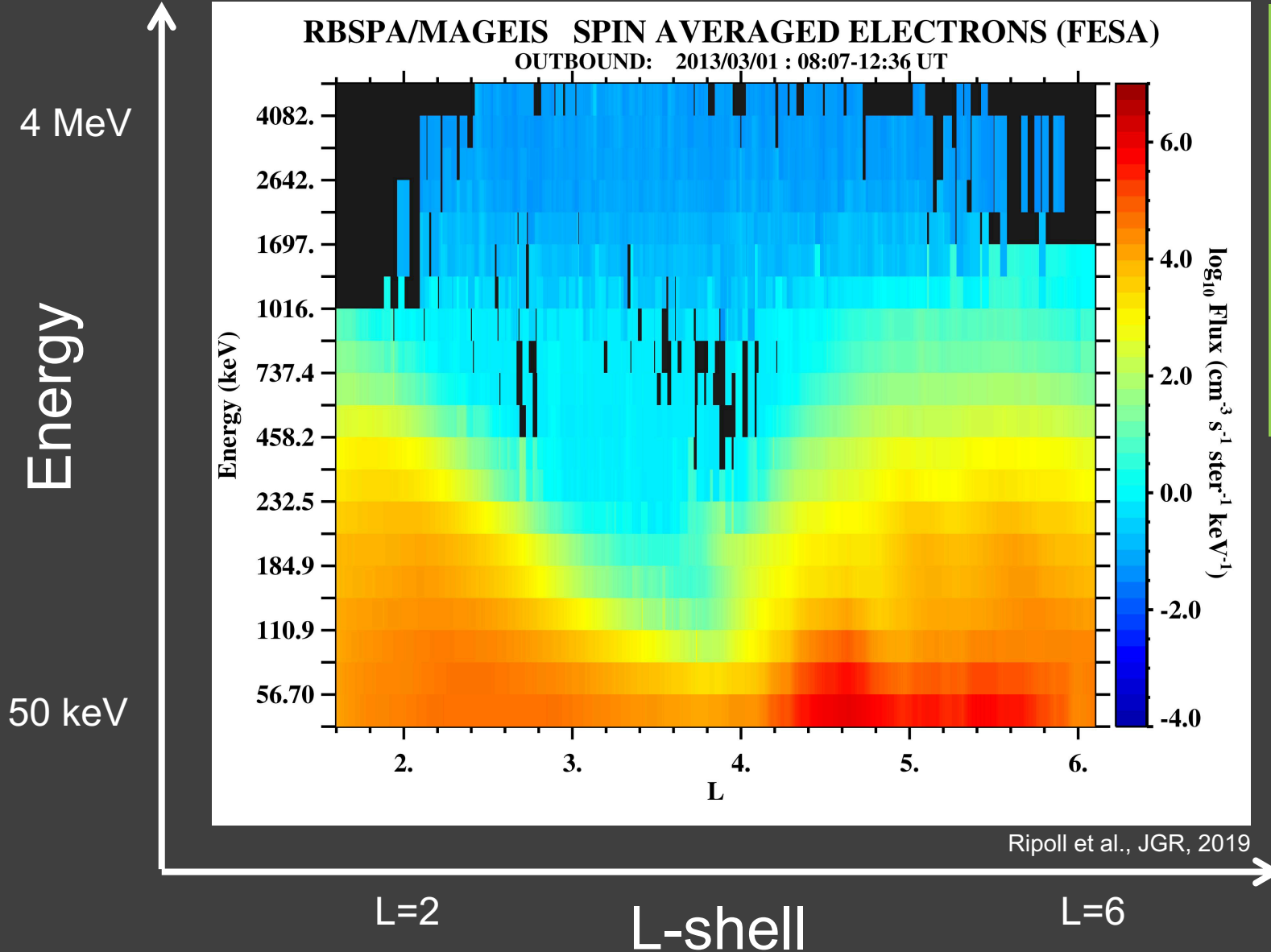


Van Allen Probes show the inner radiation zone contains no MeV electrons by Fennell et al., GRL, 2015)
The impenetrable barrier, Baker et al., Nature [2014]

- Storm and substorm injections (~250 keV Turner et al. 2015)
- Clear energy dependence of the location of the belt
- Discovery of Fennell's 2015 limit of the Inner RB at ~1 MeV
- E-structure discuss throughout the talk

Recent review of Radiation belt physics in :

Ripoll, J.-F., Claudepierre, S. G., Ukhorskiy, A. Y., Colpitts, C., Li, X., Fennell, J., & Crabtree, C. (2020). *Particle Dynamics in the Earth's Radiation Belts: Review of Current Research and Open Questions*. Journal of Geophysical Research: Space Physics, 125, e2019JA026735.



March 1st

March 16th
2013

1 image per 8h

(movie:
3 images/sec
=1day/sec)

Storm times :
March 1st-3rd

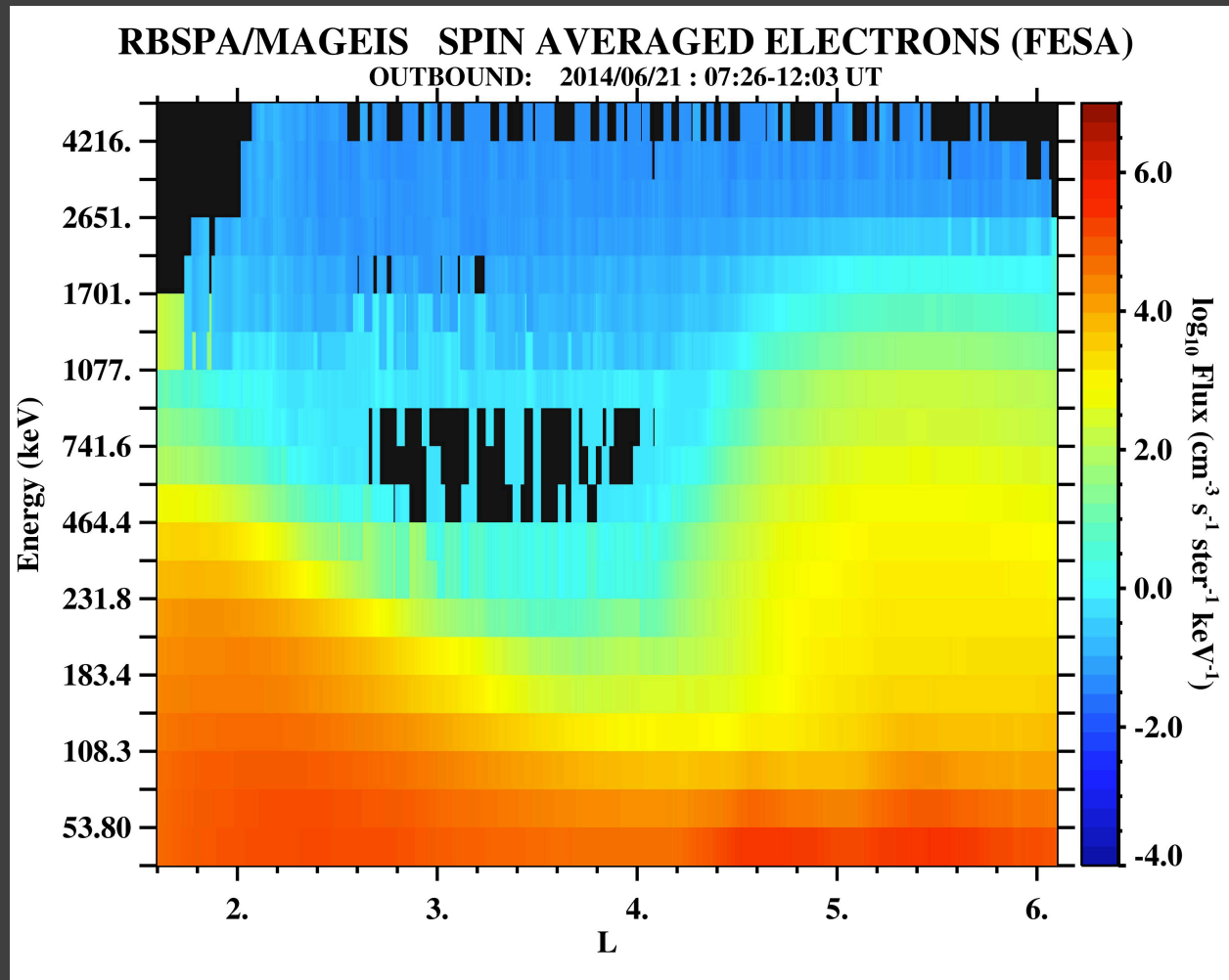
Quiet decay:
March 4th-15th

Midnight region

4 MeV

Energy

50 keV



Ripoll et al., JASTP, 2020

L=2

L-shell

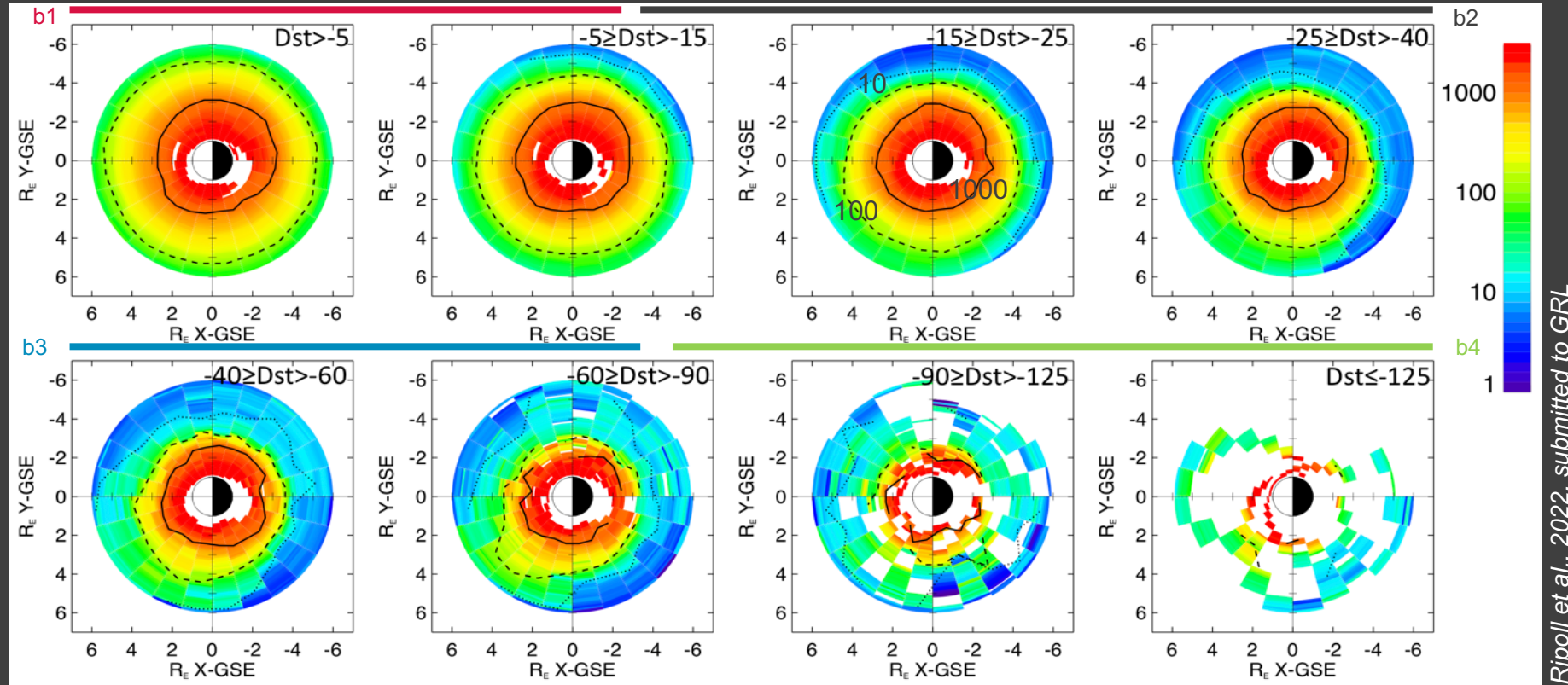
L=6

June 21st-
July 26th
2014Substorm
and HSS
injections

- Dynamic injections below 232 keV.
- Substorm injections (e.g. 3rd and 8th)
- ORB with S-shape pattern
- Slot formation
- Gradual outer belt decay

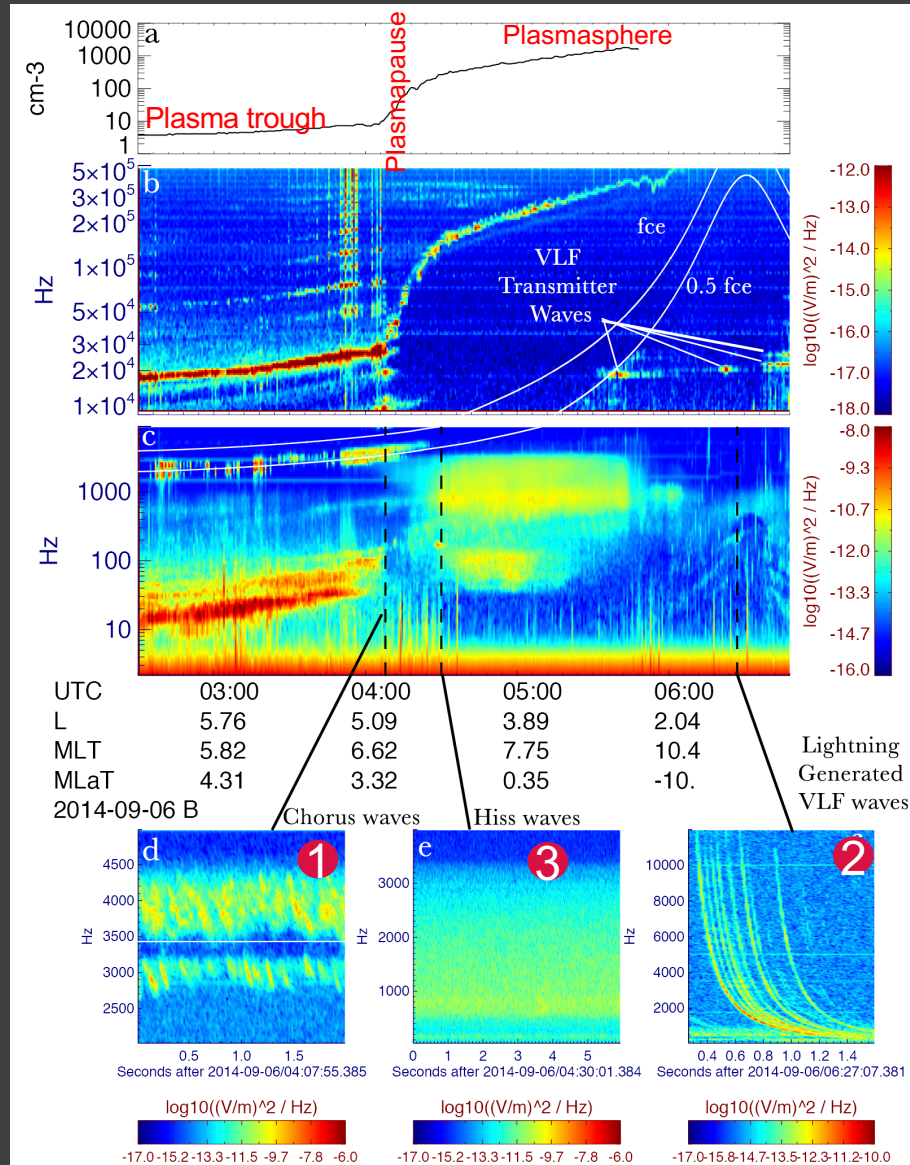


Cold electron plasma and whistler-mode waves



Ripoll et al., 2022, submitted to GRL

- Quiet times: isotropic plasmasphere extending above $L=5$ (almost $L=6$). Asymmetry forming with Dst increasing
- Plumes expanding further than $L \sim 6$
- Detached plasma pockets wrapping around the Earth between $L=4$ and $L=6$
- Loosing resolution for $Dst < -90$
- The L_{pp} as a marker of activity
- The outer electron belt lies within the plasmasphere for 40% of all times (at least for $Kp < 1$)
- 65% of any RBSP data at a given L-shell falls within the plasmasphere, versus 35% in the plasma trough.

Plasma
densityPower
Spectral
Density
(PSD)Macroscale
StructurePower
Spectral
DensityMicroscale
Structure

Most prominent waves:

- Plasmasphere with whistler mode hiss waves
- Chorus waves in the plasma trough

Less prominent waves:

- VLF Transmitter waves
- Lightning-generated whistler-waves (LGW)

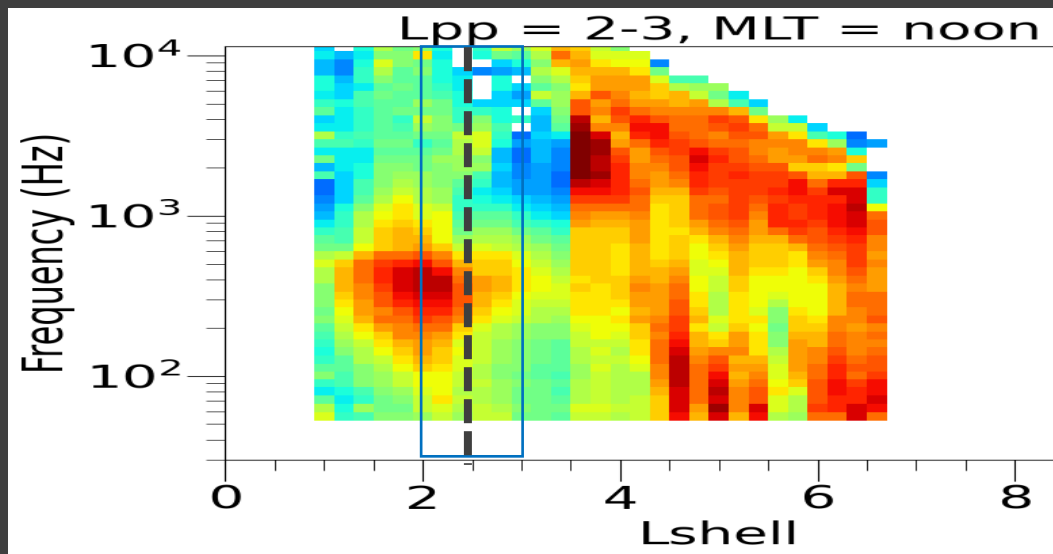
Maximum electromagnetic power

- Hiss : RMS(B)=16 pT in 10-14 MLT for 300-650 Hz from Polar satellite (Falkowski+17)
RMS(B)=38 pT all storms measured by the Van Allen Probes between 9/ 2012 and 12/2018 (Malaspina+18)
Max ~200 pT for extreme hiss in plumes (Shi+19, Millan & Ripoll 21)
- Lightning superbolt whistlers: RMS(B)~83 pT
- Chorus max. ~ 3 nT (Hospodarsky+16)
- EMICs max ~ 10 nT (Engebretson+2015)
- Whistler-mode waves (non-LGW) : RMS(E)~250 mV/m (Cattel+08)

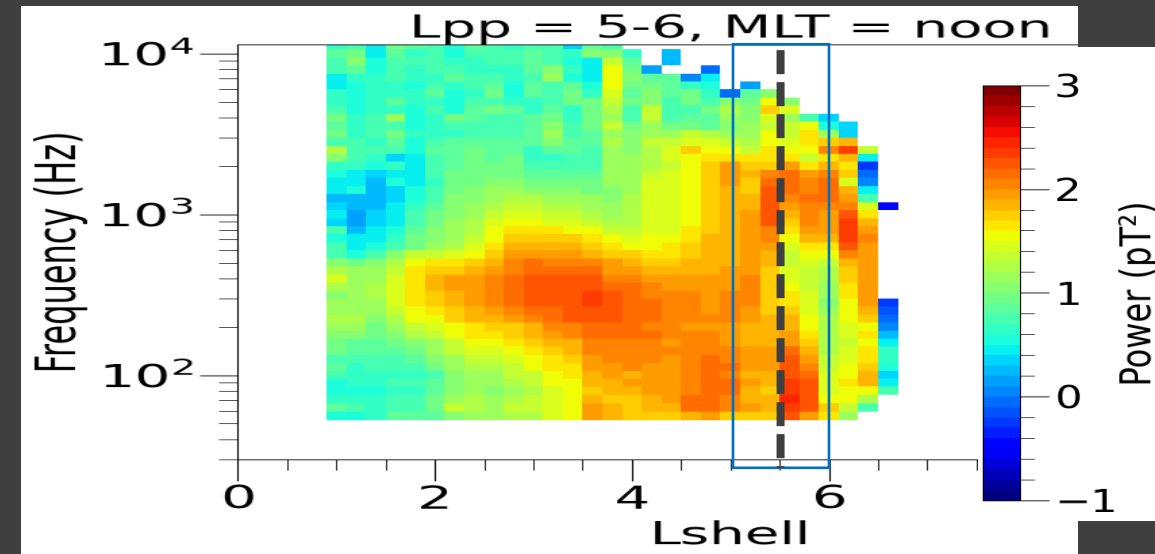
The whistler-mode statistical wave zoo system sorted by bins of plasmapause location

Extension of Malaspina et al. GRL 2017 to the whole RBSP mission

High activity ($L_{pp}=2-3$, MLT=noon)



Low activity ($L_{pp}=5-6$, MLT=noon)

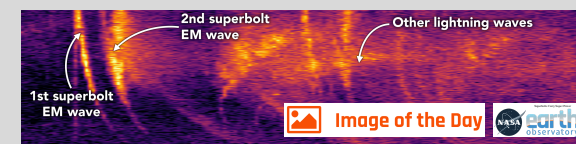


(Ripoll, Malaspina, Cunningham et al. 2021, in preparation)

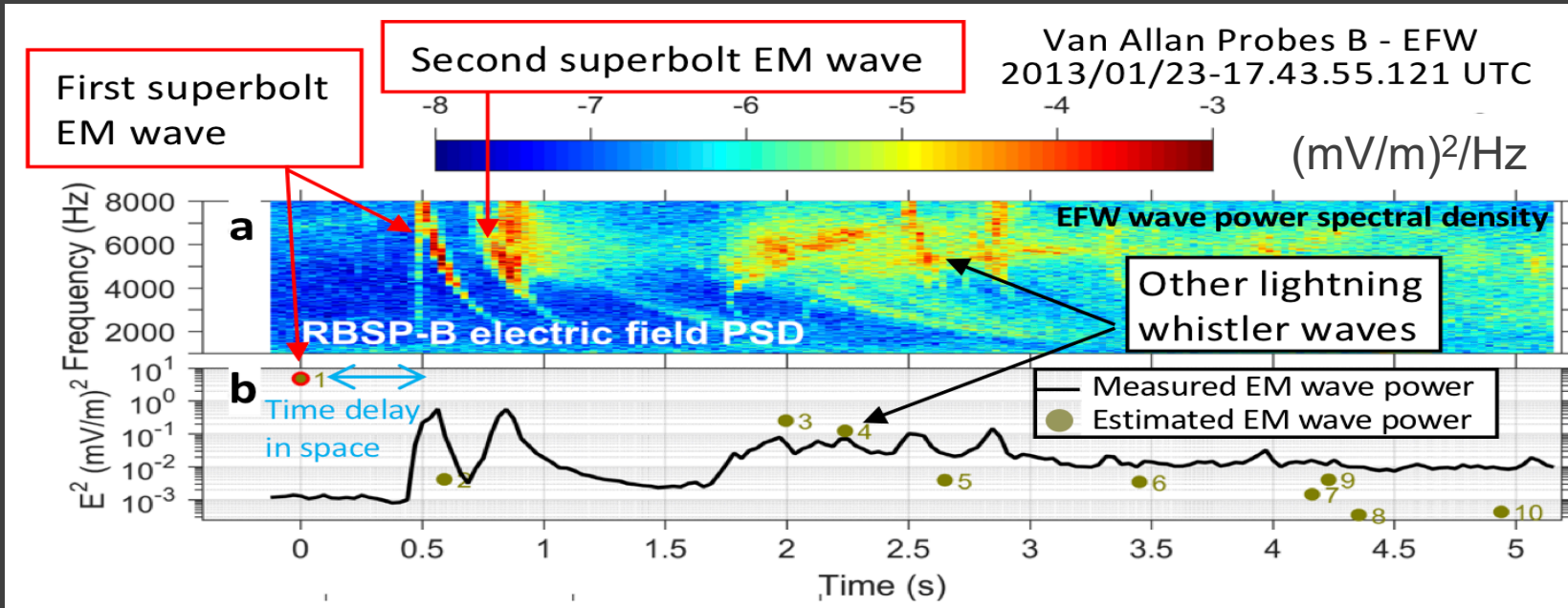
- Overlap of hiss/chorus in $L \sim 2-3$ and $L \sim 5-6$
- Importance of hiss up to $L \sim 6$ for quiet times

- Importance of plasmasphere and wave coupling
- The statistical approach mixes the effects

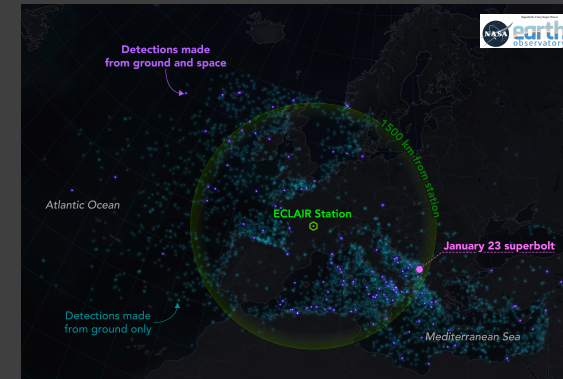
Extreme lightning-generated whistler wave (superbolt) recorded on Earth and in space



EM signal in space



Report from the ISSI Team #477 <https://www.issibern.ch/teams-electromagnetic-power/>

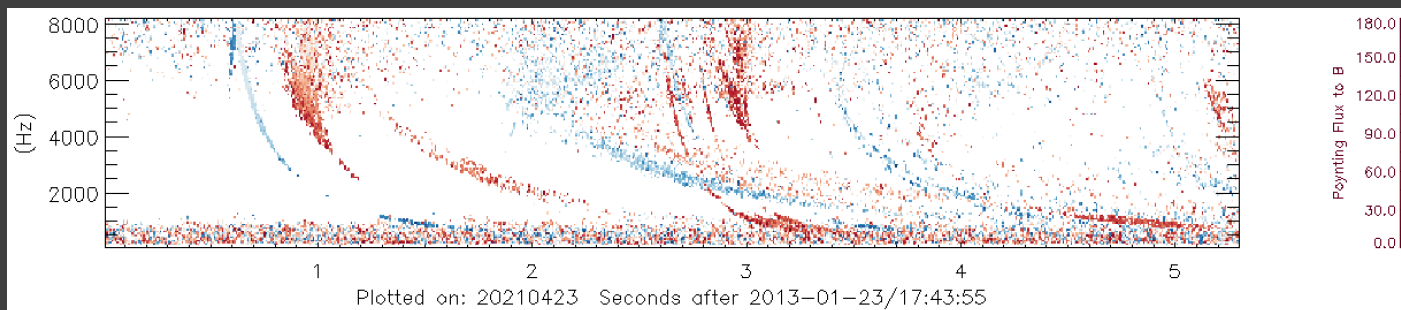


Superbolts location from WWLLN Holzworth+, GRL, 2019

→ Electric power is attenuated by ~8 orders of magnitude from Earth to space

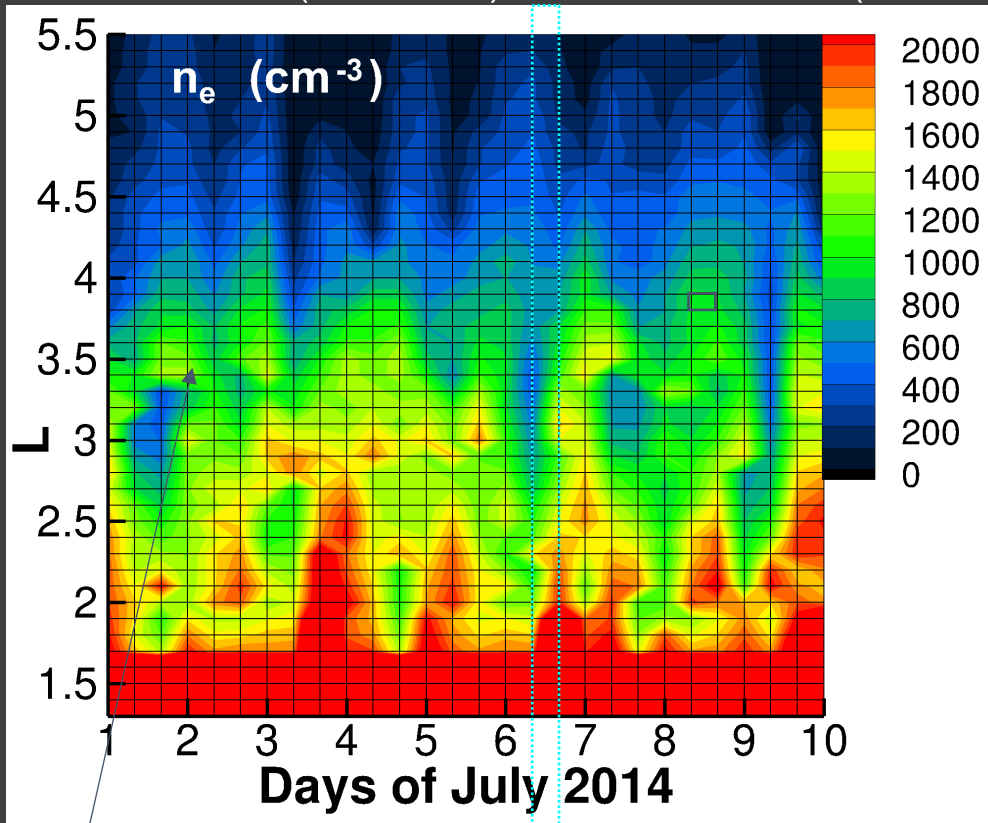
J.-F. Ripoll^{1,2,3*}, T. Farges¹, D. M. Malaspina^{3,4}, G. S. Cunningham⁵, E. H. Lay⁶, G. B. Hospodarsky⁷, C. A. Kletzing⁷, J. R. Wygant⁸ & S. Pédebois⁹

Poynting flux showing successive change of sign



Cold plasma density

data from EMFISIS (Kurth et al.) and SCC from EFW (S. Thaller, LASP)

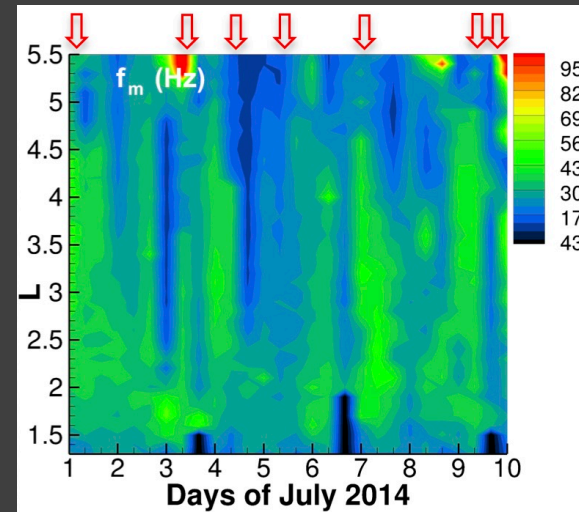


One cell of the observation/simulation

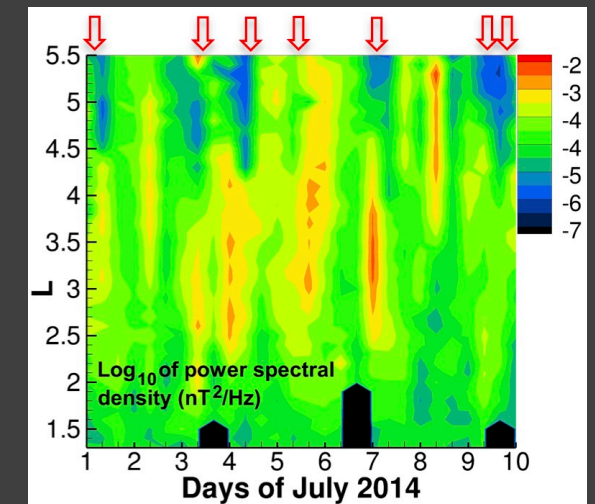
Time bin = Av. of n_e during 8 hours (~ 1 RBSP path) within $0.1L$

Whistler-mode hiss waves

Mean Hiss Frequency



Hiss Wave Power

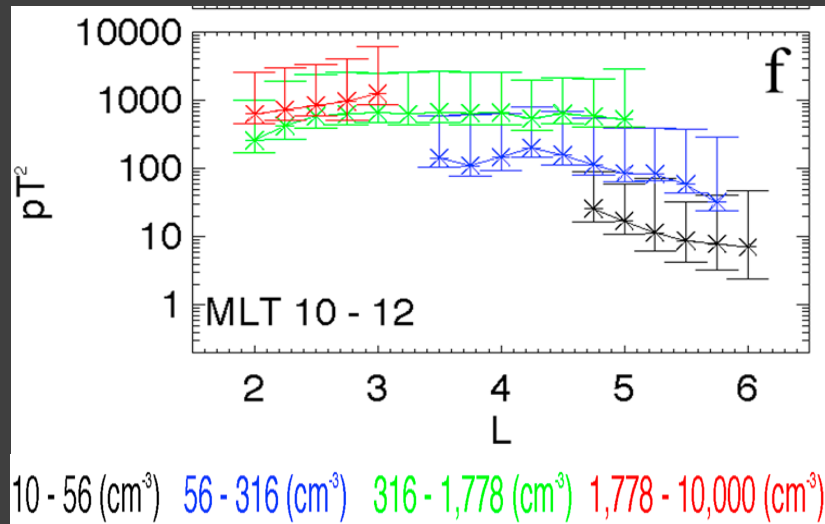


- 3 frequency populations, two for hiss (200–400 and 600–800 Hz), and chorus can be in the 1-2 kHz hiss band outside the plasmasphere
- Hiss power compressed inward during injections
- Wave amplitudes vary by orders of magnitude.
- The stronger hiss waves are located in the plasmasphere interior, between $L = 2$ and $L = 4$.
- W_{na} response not shown

Ripoll et al. 2020, JAST

High Correlation between Plasmaspheric Hiss Wave Power and Cold Plasma Density

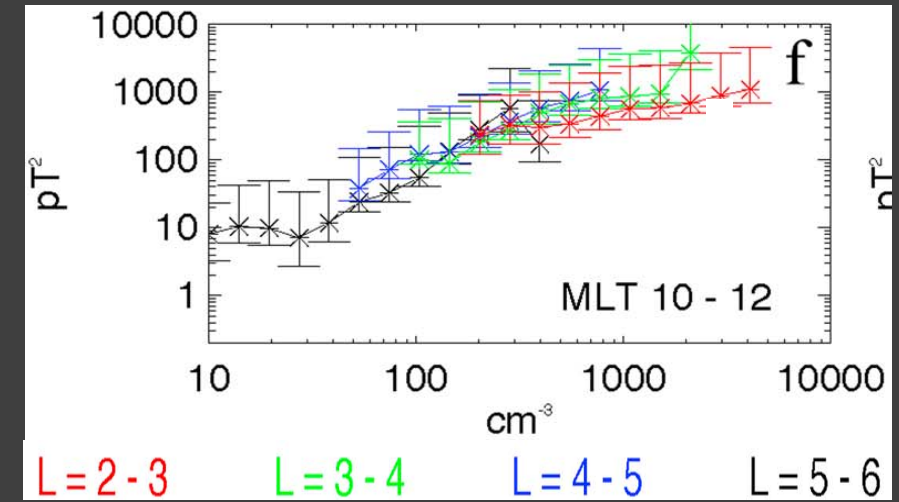
Hiss Power Sorted vs L



→ Hiss sorted with
plasmopause
location in
Malaspina et al.
GRL 2017

→ New sorting
with density

New Hiss Power Sorted vs Density



Hiss power highly correlated with density:

Plasmaspheric hiss wave power strictly increases with plasma density ($L > \sim 2.5^*$)

- This increase is stronger and occurs regardless of L and for all MLTs ($L > \sim 3$)
- These conclusions hold for variable AE*
- This correlation pleads in favor of a local generation mechanism for hiss (open subject cf. review Rad. Belt Physics, Ripoll et al. JGR 2020)

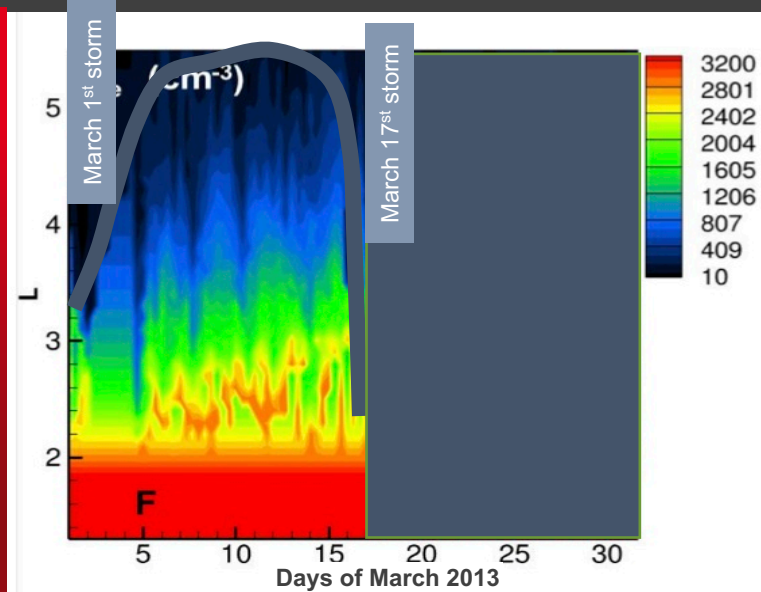
Malaspina, D. M., Ripoll, J.-F., Chu, X., Hospodarsky, G., Wygant, J. (2018). Variation in plasmaspheric hiss wave power with plasma density. Geophysical Research Letters, 45. <https://doi.org/10.1029/2018GL078564>



Fokker-Planck modeling, event-driven wave-particle interactions and simulations of the radiation belt dynamics

During quiet times, the plasmasphere extends above L=5.

Electron density ($\#/cm^{-3}$)



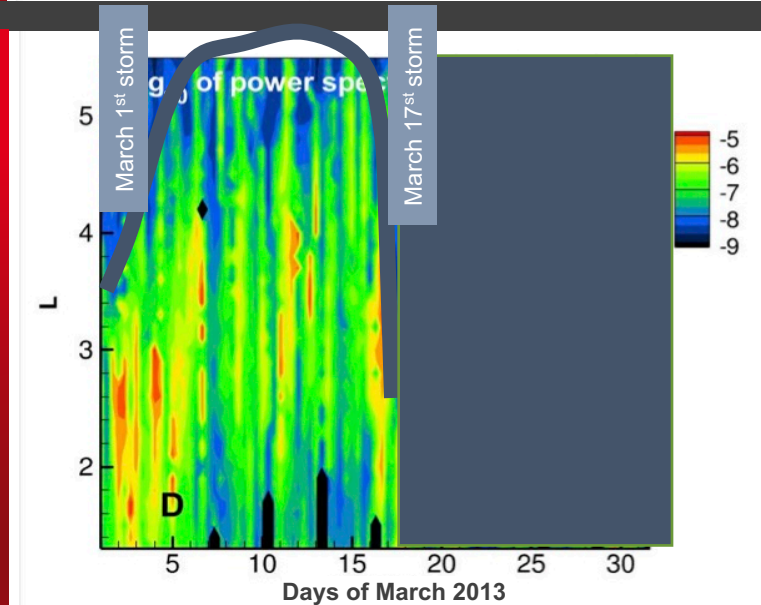
Density EMFISIS (Kurth et al.) and SCC from EFW (S. Thaller, UM)

Wave frequencies and wave normal angle from EMFISIS (compilation Santolik et al.)

Amplitudes vary by orders of magnitude, with stronger waves in the plasmasphere (L=2-4)

MLT-dependence is modeled from Spasojevic et al. 2015

Mean hiss power (nT^2/Hz)



A quite extended plasmasphere favors the existence and the effect of hiss waves

Fokker-Planck 3D: evolution of an electron at (t, L, E, α)

$$\frac{\partial f}{\partial t} = L^2 \frac{\partial}{\partial L} \left(\frac{D_{LL}}{L^2} \frac{\partial f}{\partial L} \right) + \frac{1}{p^2} \frac{\partial}{\partial p} \left(p^2 D_{pp} \frac{\partial f}{\partial p} \right) + \frac{1}{G} \frac{\partial}{\partial \alpha} \left(G D_{\alpha\alpha} \frac{\partial f}{\partial \alpha} \right)$$

+
Cross-terms
neglected

Evolution of the electron distribution function

Transport of the electron from WPI by ULF waves

Acceleration of the electron from WPI by VLF waves

Scattering of the electron from WPI by VLF waves

The scattering of an electron at (L, E, α, t) by an electromagnetic wave (here LGW) is caused by pitch angle diffusion: $D_{\alpha\alpha}(L, E, \alpha, t)$

$$D_{\alpha\alpha}(L, E, \alpha, t) = B_{LGW}^2 \times P(f) \times P(\theta) \times F(B_{mag}(L), E, \alpha, f_{res})$$

Wave properties

- frequency distribution
- wave normal angle distribution
- wave power

- electron properties and resonance
- ambient mag. field
- cold plasma density

We compute an event-driven pitch angle diffusion coefficient from all wave/plasma properties from RBSP: 8h resolution, 0.1L. 50 harmonics. Non-//.

$$\overset{\text{8h-resolved}}{D_{\alpha\alpha}(\omega_m, \theta_m, n_e)} \longrightarrow \overset{\text{Time-averaged}}{D_{\alpha\alpha}(\omega_m, \theta_m, n_e)}$$

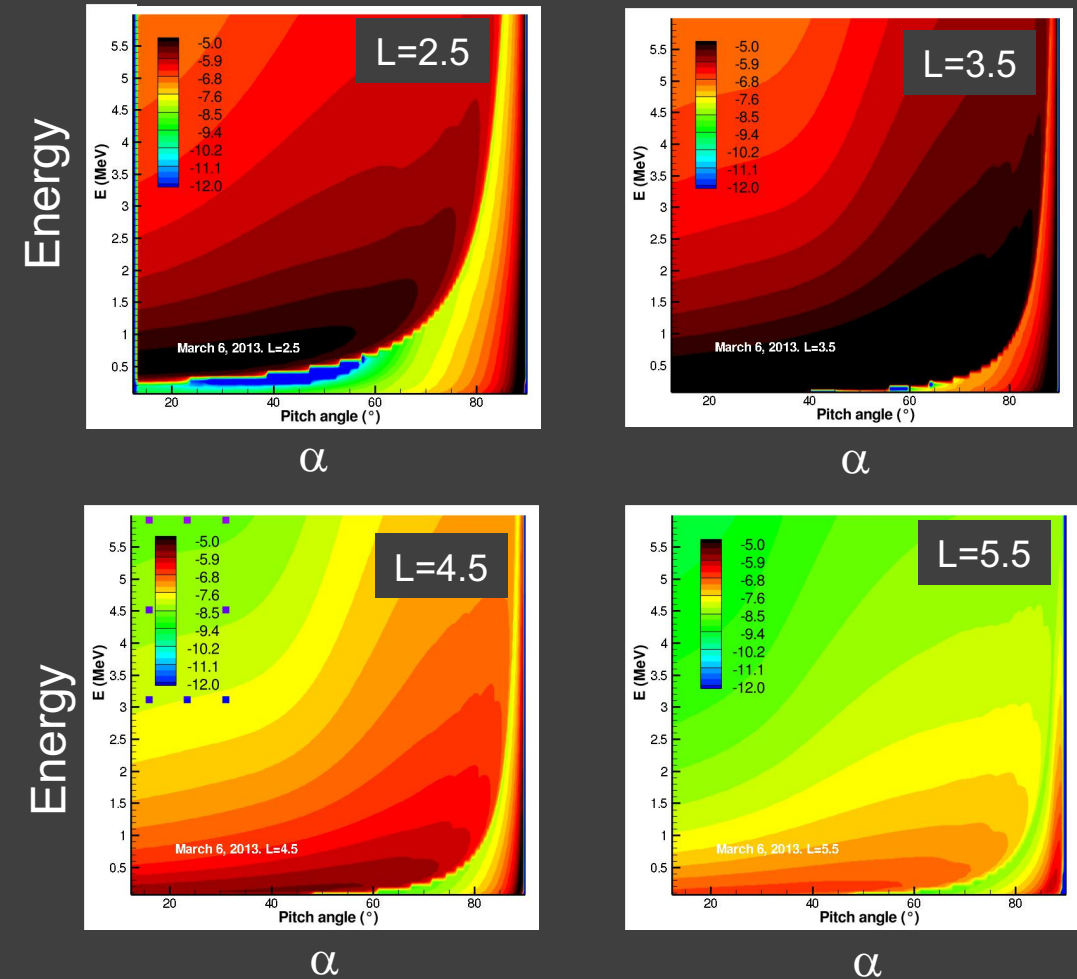
Not doing

~~$$D_{\alpha\alpha}(\omega_m, \theta_m, n_e)$$~~

From Watt et al. GRL 2021:

- Numerical diffusion experiments are sensitive to variability time scales, even at same time-integrated diffusion
- Experiments reveal more diffusion from average of all diffusion coefficients than when coefficient is constructed from averaged inputs

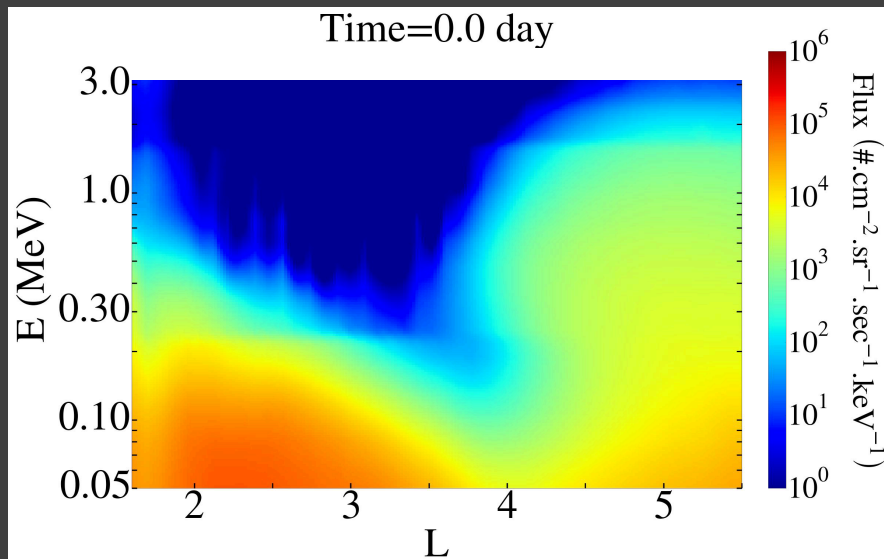
Pitch angle diffusion coefficients $D_{\alpha_0\alpha_0}$ for 6th of March 2013



Ripoll et al., JGR, 2017

Massively parallel computations for 6×10^7 $D_{\alpha_0\alpha_0}(L, t, E, \alpha_0)$. (4 years 1 proc)

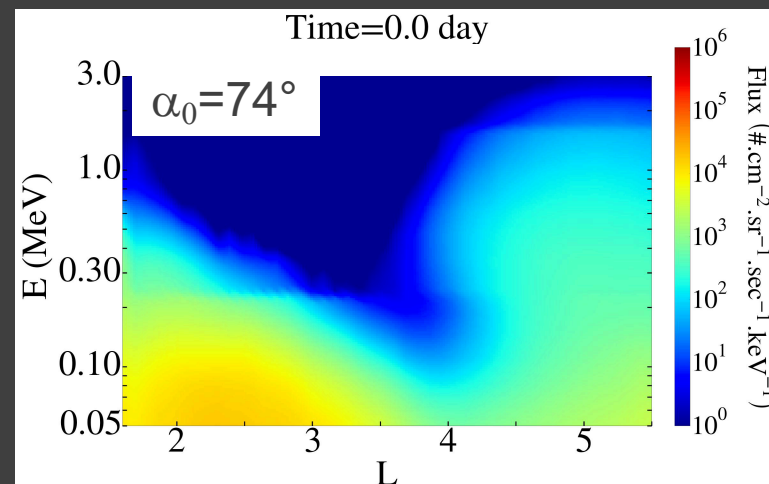
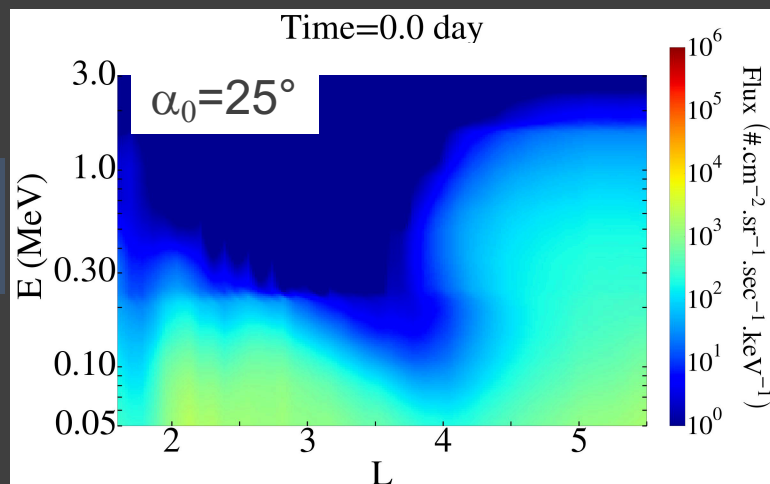
Omni-Flux



Method

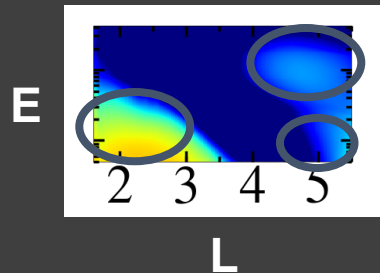
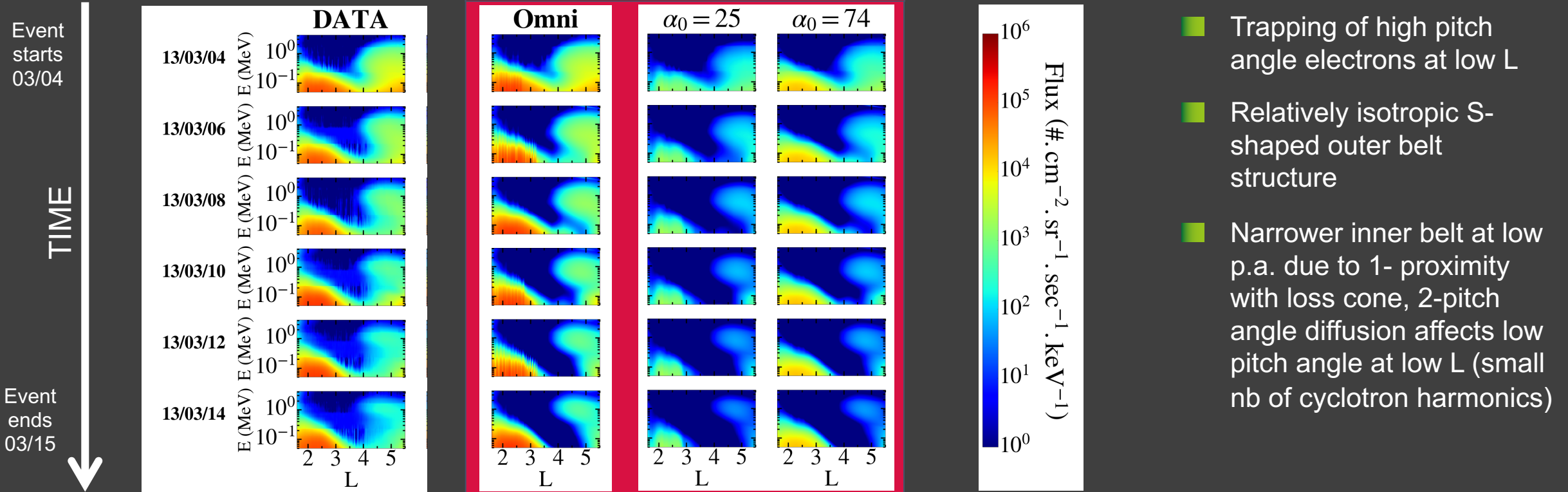
- Solving for RD+PAD from Hiss
- Verb3D-skeleton (v. 2.4.2) for solving radial & p.a. diffusion
- $D_{\alpha\alpha}$ of this work
- BC & IC from MagEIS
- Omniflux is integral of unidir. flux at the latitude of RBSP

Unidirectional Flux



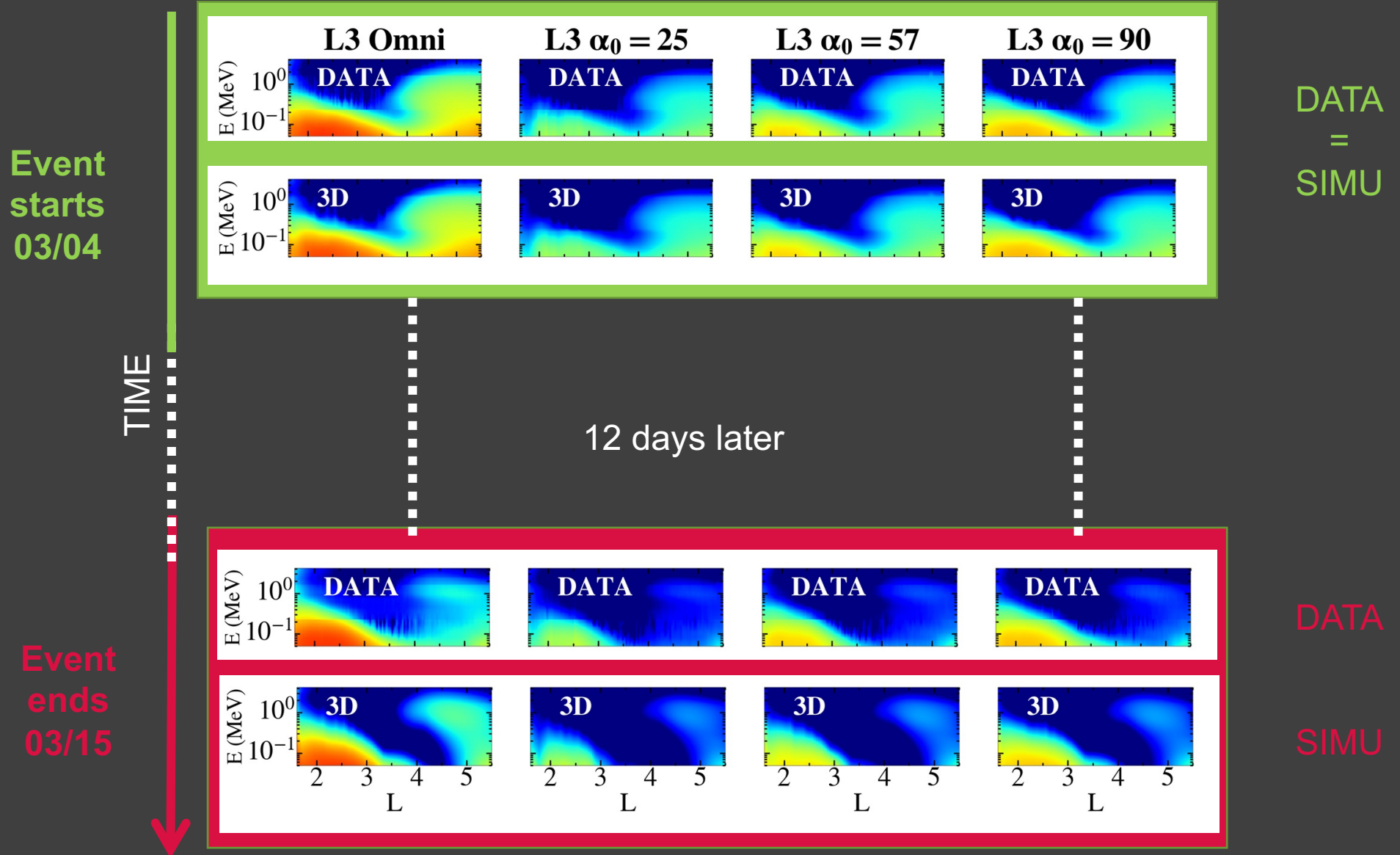
Van Allen Probes/MagEIS

VERB-3D simulations



The 3 preserved zones from hiss

- Inner belt
- Outer low energy seed population
- Outer MeVich *pocket* or *island*





Conclusions and Perspectives

- Ongoing work to build whistler-mode wave statistics and databases of typical events from RBSP
- The plasmasphere expands further than expected from seminal models during quiet times as well as storms (by $\sim 0.5L$) (Ripoll+, submitted to GRL, 2022)
- Hiss dependence on density (fundamental for their origins). Importance of the coupling for RB simulations

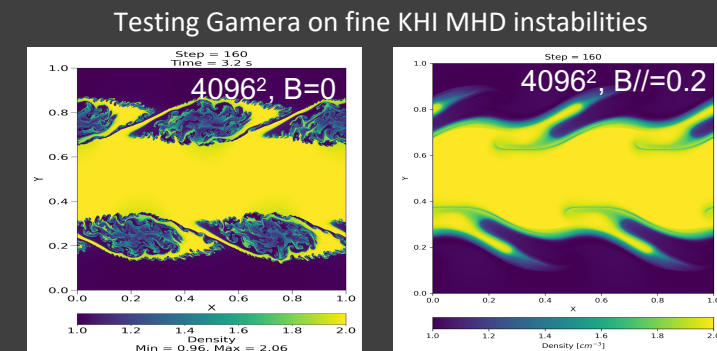
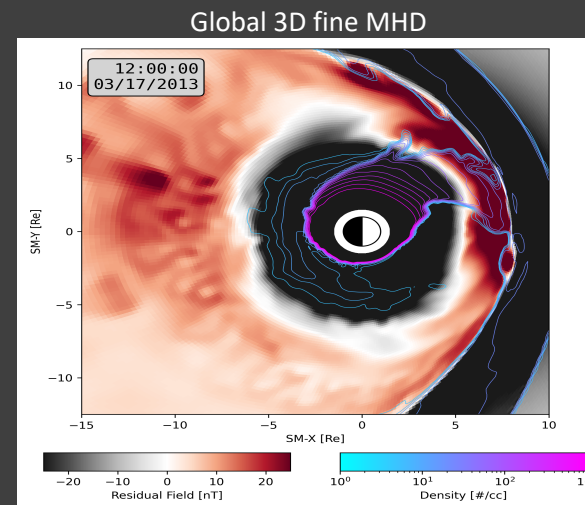
- The plasmasphere through plasmaspheric waves plays an important role in the dynamics of the outer belt (Ripoll+16, 19, 20)
 - The outer electron belt lies within the plasmasphere for 40% of all times (i.e. $Kp < 1$).
 - 65% of any RBSP data at a given L-shell falls within the plasmasphere, versus 35% in the plasma trough.

- Fokker-Planck simulations reproduce the RB energy structure for quiet times and moderate substorm activity (event-driven for conserving couplings)

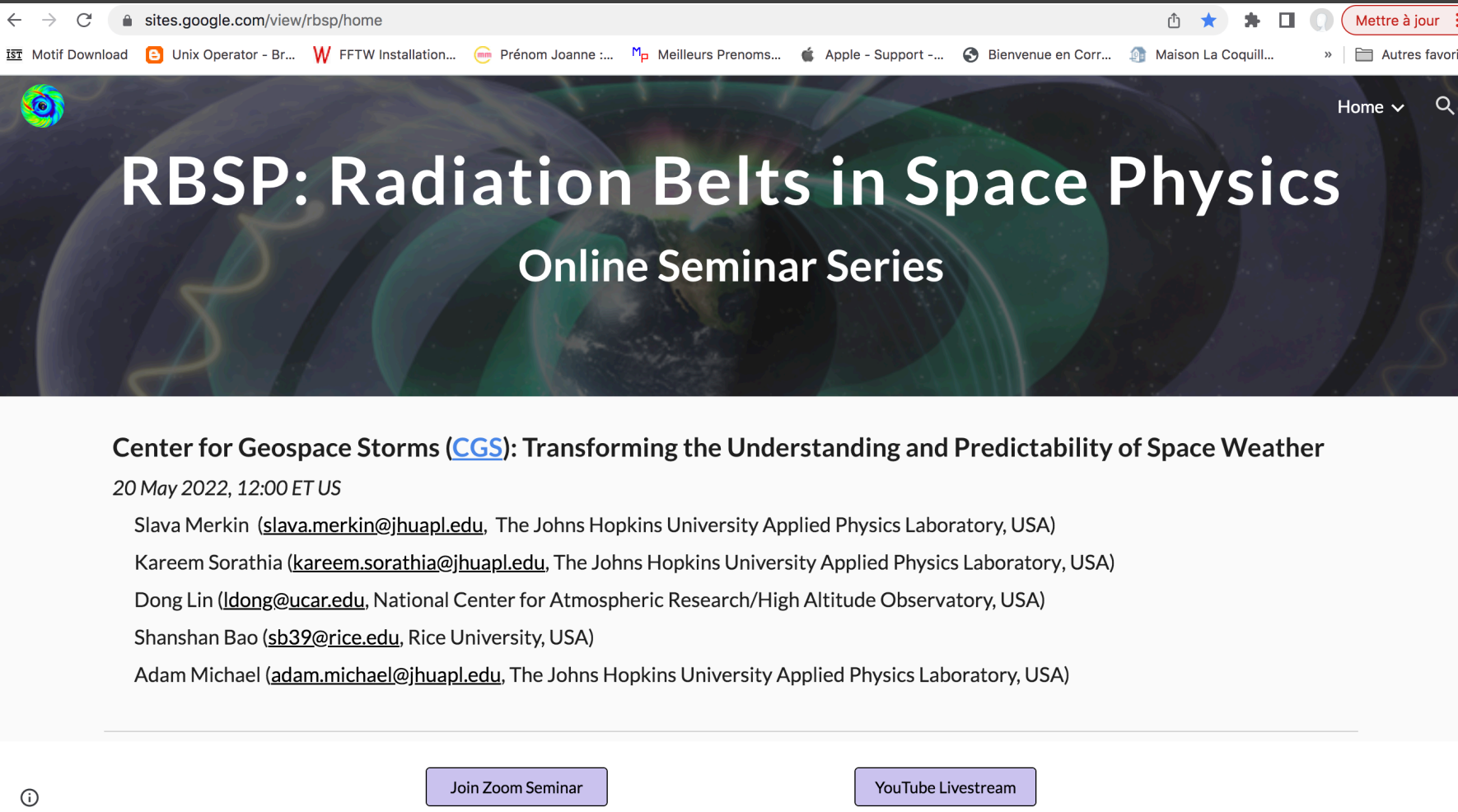
- New generation of radiation belt codes : global MHD codes + QL WPI + plasmasphere models should really change our global understanding.

Global MHD codes with coupled plasmasphere with APL/Gamer). APL team: Sorathia-Merkin-Ukhorskiy

Thèse M. Cosmides at CEA (2020-2023)



- Ripoll, J.-F., Claudepierre, S. G., Ukhorskiy, A. Y., Colpitts, C., Li, X., Fennell, J., & Crabtree, C. (2020). *Particle Dynamics in the Earth's Radiation Belts: Review of Current Research and Open Questions*. *Journal of Geophysical Research: Space Physics*, 125, e2019JA026735.
- Pierrard, V., Ripoll, J.-F., Cunningham, G., Botek, E., Santolík, O., Thaller, S., et al. (2021). *Observations and simulations of dropout events and flux decays in October 2013: Comparing MEO equatorial with LEO polar orbit*. *Journal of Geophysical Research: Space Physics*, 126, e2020JA028850.
- Ripoll, J.-F., M. H. Denton, D. P. Hartley, G. D. Reeves, D. Malaspina, G. S. Cunningham, O. Santolík, S. A. Thaller, et al. (2020), *Scattering by whistler-mode waves during a quiet period perturbed by substorm activity*, *Journal of Atmospheric and Solar–Terrestrial Physics*
- Ripoll, J.-F., Loridan, V., Denton, M. H., Cunningham, G., Reeves, G., Santolík, O., et al. (2019). *Observations and Fokker-Planck simulations of the L-shell, energy, and pitch angle structure of Earth's electron radiation belts during quiet times*. *Journal of Geophysical Research: Space Physics*, 124.
- Malaspina, D. M., Ripoll, J.-F., Chu, X., Hospodarsky, G., Wygant, J. (2018). *Variation in plasmaspheric hiss wave power with plasma density*. *Geophysical Research Letters*, 45.
- Ripoll, J.-F., O. Santolík, G. D. Reeves, W. S. Kurth, M. H. Denton, V. Loridan, S. A. Thaller, C. A. Kletzing, and D. L. Turner (2017), *Effects of whistler mode hiss waves in March 2013*, *J. Geophys. Res. Space Physics* 122.
- Ripoll, J.-F., G. Reeves, G. Cunningham, V. Loridan, M. Denton, O. Santolík, W. S. Kurth, C. A. Kletzing, D. L. Turner, M. G. Henderson, A. Y. Ukhorskiy (2016), *Reproducing the observed energy-dependent structure of Earth's electron radiation belts during storm recovery with an event-specific diffusion model*, *Geophysical Research Letters*.
- Ripoll J.-F., Farges, T., Malaspina, D.M., Cunningham, G. S., Lay, E. H. et al. *Electromagnetic power of lightning superbolts from Earth to space*. *Nature Communications* 12, 3553 (2021). <https://doi.org/10.1038/s41467-021-23740-6>
- Ripoll, J.-F., Farges, T., Malaspina, D. M., Lay, E. H., Cunningham, G. S., Hospodarsky, G. B., et al. (2020). *Analysis of electric and magnetic lightning-generated wave amplitudes measured by the Van Allen Probes*. *Geophysical Research Letters*, 47, e2020GL087503. <https://doi.org/10.1029/2020GL087503>



sites.google.com/view/rbsp/home

Home

RBSP: Radiation Belts in Space Physics

Online Seminar Series

Center for Geospace Storms (CGS): Transforming the Understanding and Predictability of Space Weather

20 May 2022, 12:00 ET US

Slava Merkin (slava.merkin@jhuapl.edu, The Johns Hopkins University Applied Physics Laboratory, USA)

Kareem Sorathia (kareem.sorathia@jhuapl.edu, The Johns Hopkins University Applied Physics Laboratory, USA)

Dong Lin (ldong@ucar.edu, National Center for Atmospheric Research/High Altitude Observatory, USA)

Shanshan Bao (sb39@rice.edu, Rice University, USA)

Adam Michael (adam.michael@jhuapl.edu, The Johns Hopkins University Applied Physics Laboratory, USA)

Join Zoom Seminar

YouTube Livestream

- RB physics
- Magnetospheric physics
- All planets
- Space weather

RBSP Science Organizing Committee:

Lauren Blum lauren.blum@lasp.colorado.edu

Wen Li wenli77@bu.edu

Yoshi Miyoshi miyoshi@isee.nagoya-u.ac.jp

Kyle Murphy kylemurphy.spacephys@gmail.com

Jean-Francois Ripoll jean-francois.ripoll@cea.fr

Sasha Ukhorskiy sasha.ukhorskiy@jhuapl.edu

The CEA logo, consisting of the lowercase letters 'cea' in a white, rounded, sans-serif font, positioned above a solid green horizontal line. The logo is centered within a red square that has a subtle pattern of small white dots.

cea

Merci de votre attention